Available online at www.sciencedirect.com
SCIENCE DIRECT
Polymer 47 (2006) 5323–5329
polymer
www.elsevier.com/locate/polymer

# Polymeric nanocomposite films from functionalized vs suspended single-walled carbon nanotubes

Bing Zhou [a], Yi Lin [a], Darron E. Hill [a], Wei Wang [a], L. Monica Veca [a], Liangwei Qu [a], Pankaj Pathak [a], Mohammed J. Meziani [a], Julian Diaz [a], John W. Connell [b], Kent A. Watson [c], Lawrence F. Allard [d], Ya-Ping Sun [a,*]

[a] *Department of Chemistry and Laboratory for Emerging Materials and Technology, Clemson University, Clemson, SC 29634-0973, USA*
[b] *NASA Langley Research Center, Advanced Materials and Processing Branch, Hampton, VA 23681-2199, USA*
[c] *National Institute of Aerospace, 100 Exploration Way, Hampton, VA 23666-6147, USA*
[d] *High Temperature Materials Laboratory, Oak Ridge National Laboratory, Oak Ridge, TN 37831-6062, USA*

Received 16 April 2006; received in revised form 17 May 2006; accepted 19 May 2006
Available online 12 June 2006

**Abstract**

The reported work was to demonstrate that the defect-derived photoluminescence in functionalized single-walled carbon nanotubes could be exploited in probing the dispersion of these nanotubes in polymeric nanocomposites because the luminescence emissions are sensitive to the degree of nanotube bundling and surface modification. The polyimide–SWNT nanocomposite thin films obtained from nanotubes with and without functionalization were compared. The spectroscopic results suggest that despite a similar visual appearance in the two kinds of films, the nanotube dispersion must be significantly better in the film with functionalized nanotubes, as reflected by the strong photoluminescence. In fact, the nanotubes embedded in polymer matrix that can be readily characterized by Raman spectroscopy are non-luminescent, while those that are difficult for Raman are strongly luminescent. Therefore, Raman and photoluminescence serve as complementary tools in the investigation of nanocomposites concerning the nanotube dispersion-related properties.


*Keywords:* Carbon nanotubes; Nanocomposites; Photoluminescence

## 1. Introduction

Polymeric nanocomposites with single-walled carbon nanotubes (SWNTs) as fillers have received much recent attention for their widely predicted superior electronic, thermal, and mechanical properties [1–3]. An important issue in the development of such nanocomposites is the dispersion of SWNTs, since as-produced SWNTs are severely bundled and entangled due largely to the strong inter-tube van der Waals interactions [1]. There is hardly any solubility of the nanotubes in common solvents, which substantially impairs their processibility. Thus, the direct incorporation of as-produced SWNTs into polymer matrices usually results in poor nanotube dispersion in the nanocomposites, with the actual performance significantly worse than expected [4]. In order to improve the dispersion, so as to maximize the transformation of the nanotube properties to the resulting nanocomposites, the functionalization of SWNTs has been identified as an effective approach [3–6]. For example, Lin et al. reported that poly(vinyl alcohol) (PVA) could be used to functionalize SWNTs for their exfoliation and solubilization and that the functionalized nanotube sample could be homogeneously dispersed into PVA matrix for high-quality nanocomposites without introducing any unwanted foreign materials [7].

In a different approach, selected polymers and common surfactant molecules have been used to aid the suspension of SWNTs in various solvents [8–10]. It has been shown that polyimide is particularly effective in stabilizing the nanotube suspension, and the resulting suspension can be used to fabricate polyimide–SWNT nanocomposites, which are also free from other agents [11]. The nanocomposites thus prepared are visually similar to those obtained from functionalized nanotube samples, despite their expected significant difference with respect to the dispersion of the embedded SWNTs.

* Corresponding author. Tel.: +1 864 656 5026; fax: +1 864 656 5007.
*E-mail address:* syaping@clemson.edu (Y.-P. Sun).

0032-3861/$ - see front matter © 2006 Elsevier Ltd. All rights reserved.
doi:10.1016/j.polymer.2006.05.055

Commonly employed nanoscale characterization techniques such as high-resolution electron microscopy may in principle be applied to an evaluation of the dispersion issue, though the preparation of specimens for the microscopy analyses can be challenging. For example, the microtome process to obtain ultra-thin slices of the nanocomposite often distorts the original distribution of embedded nanotubes in the polymer matrix [12]. As a result, optical spectroscopy methods including especially Raman are widely pursued for the characterization of polymer–SWNT nanocomposites in a convenient and rapid fashion [13–15]. However, Raman is not so useful in the investigation of nanocomposites obtained from homogeneously dispersed functionalized carbon nanotubes because of overwhelming interference of photoluminescence from these nanotubes [6,16].

In this work, we wanted to demonstrate that the photoluminescence in functionalized SWNTs could be exploited in probing the dispersion of these nanotubes in polymeric nanocomposites because the luminescence emissions are sensitive to the degree of nanotube bundling and surface modification. In fact, the nanotubes embedded in polymer matrix that can be readily characterized by Raman are non-luminescent, while those that are difficult for Raman are strongly photoluminescent. Therefore, Raman and photoluminescence may serve as complementary tools in the investigation of nanocomposites concerning the nanotube dispersion-related properties. The polyimide–SWNT nanocomposite films obtained from nanotubes with and without functionalization are compared. The films have also been analyzed by electron microscopy techniques to support the spectroscopic results.

## 2. Experimental section

### 2.1. Materials

4,4′-(Hexafluoroisopropylidene)diphthalic anhydride (99%) was purchased from Aldrich, 1,3-bis-(3-aminophenoxy)benzene (96%) from TCI, and 1-ethyl-3-(3-(dimethylamino)-propyl)carbodiimide hydrochloride (EDAC, 98+%) from Alfa Aesar. Dimethylformamide (DMF) and other solvents were obtained from Mallinckrodt and carefully distilled before use. The polyimide based on 4,4′-(hexafluoroisopropylidene)-diphthalic anhydride and 1,3-bis-(3-aminophenoxy)benzene (also known as LaRC CP-2™ or simply CP-2) was supplied by SRS, Inc. According to GPC analysis (linear polystyrene standards), the polymer molecular weight $M_n$ was ~17,000 and polydispersity index ~3.

The sample of SWNTs (from the arc-discharge method) was purchased from Carbon Solutions, Inc. It was purified by using a combination of thermal oxidation and diluted nitric acid treatment, as already reported in the literature [17].

### 2.2. Measurements

UV/vis/near-IR absorption spectra were recorded on Shimadzu UV3100 spectrophotometer. Raman spectra were obtained on a Jobin Yvon T64000 spectrometer equipped with a Melles-Griot 35 mW He–Ne laser source for 632.8 nm excitation, a triple monochromator, a research grade Olympus BX-41 microscope, and a liquid-nitrogen-cooled Symphony detector. Luminescence emission spectra were measured on a Spex Fluorolog-2 emission spectrometer equipped with a 450 W xenon source, a Spex 340S dual-grating and dual-exit emission monochromator, and two detectors. The two gratings are blazed at 500 nm (1200 grooves/mm) and 1000 nm (600 grooves/mm). The room-temperature detector consists of a Hamamatsu R928P photomultiplier tube operated at 950 V, and the thermoelectrically cooled detector consists of a near-IR sensitive Hamamatsu R5108 photomultiplier tube operated at 1500 V. Unless specified otherwise, the reported spectra were corrected for non-linear instrumental response by use of predetermined emission correction factors. Scanning (SEM) and transmission (TEM) electron microscopy images were obtained on a Hitachi S4700 field-emission SEM system and a Hitachi HF-2000 TEM system, respectively. Composite film specimens for SEM imaging were subject to platinum sputtering for 60 s in order to suppress surface charging effect. The film thickness was measured by using a Nikon Digimicro Stand MS-11C with a MFC-101 digital display device.

### 2.3. PI-$NH_2$ and PI-$NH_2$–SWNT

Amine-terminated polyimide (PI-$NH_2$) was synthesized in conventional condensation polymerization of 1,3-bis(3-aminophenoxy)benzene and 4,4′-(hexafluoroisopropylidene)-diphthalic anhydride with a calculated excess of the former to ensure the amino group termination and the control of the polymer molecular weight to approximately 5000 [18]. The functionalization of SWNTs by PI-$NH_2$ was achieved in carbodiimide (EDAC)-activated amidation reaction of the terminal amino groups in PI-$NH_2$ with the defect-derived carboxylic acid groups on the nanotube surface, as reported previously [18] (Scheme 1).

### 2.4. Nanocomposite films

For film with suspended SWNTs, a purified SWNT sample (5 mg) was suspended in DMF (3 mL) and homogenized (PowerGen 125) for 1 h under flowing $N_2$. A DMF solution of the CP-2 polyimide (4 mL, 125 mg/mL) was added to the nanotube suspension under constant stirring, and the mixture was sonicated (VWR Aquasonic 150 HT) for 12 h. The resulting suspension was further stirred to slowly evaporate the solvent until the total volume reduced to approximately 2 mL. The viscous suspension thus obtained was cast onto a glass substrate with an adjustable film applicator (Gardco), and kept in flowing $N_2$ for 24 h. The film was further cured under the same atmosphere at 100 °C for 1 h, 150 °C for 1 h, 200 °C for 1 h, and finally dried in vacuum at 60 °C for 48 h.

For film with functionalized SWNTs, a DMF solution of PI-$NH_2$–SWNT (3 mL, 33 mg/mL) was added dropwise to a DMF solution of CP-2 (4 mL, 500 mg/mL) under constant stirring. The mixture was vigorously agitated until

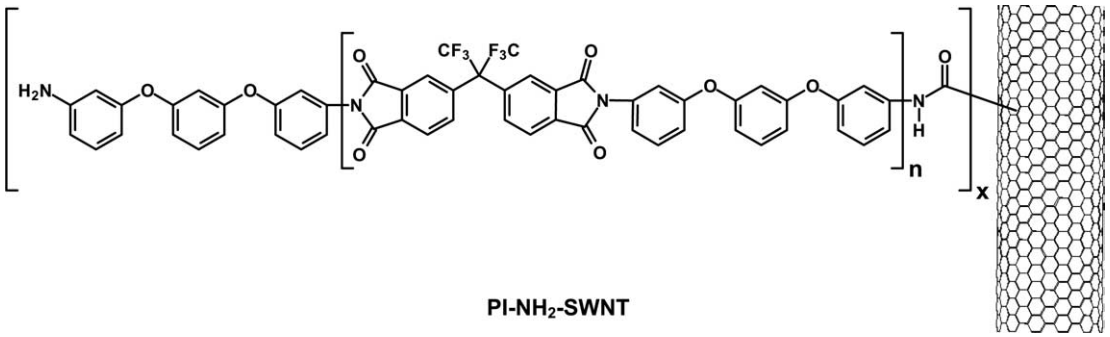


Scheme 1.

homogeneous, followed by essentially the same casting and drying procedures as described above.

## 3. Results and discussion

### 3.1. Purification and functionalization of SWNTs

The commercially available SWNT sample was purified by using an established procedure of first heat treatment (300 °C) in air and then refluxing in diluted nitric acid (2.6 M) to remove amorphous carbonaceous impurities and residual metal catalysts from the sample [17]. According to discussion in the literature concerning the effectiveness of the procedure [19,20], the purification should be adequate for the purpose of preparing polymeric nanocomposites used in this work.

The purified SWNT sample was used in the functionalization with PI-$NH_2$. The target of functionalization was the amidation of nanotube-bound carboxylic acid groups, which are known to be present in the oxidative acid-treated sample [6,21]. The functionalized nanotube sample PI-$NH_2$–SWNT was characterized by using various instrumental techniques to have the results calibrated with those reported previously [18]. For example, the $^1$H NMR signals of the terminal aniline aromatic protons in PI-$NH_2$–SWNT were at 5.9–6.1 ppm, shifted upfield from those in the PI-$NH_2$ spectrum (6.0–6.4 ppm) due to effects of the large aromatic ring currents in the attached carbon nanotubes [18]. The PI-$NH_2$–SWNT sample was readily soluble in many organic solvents including THF and DMF to form dark-colored solutions. The solution-phase optical absorption spectrum of the sample in DMF exhibited features at $\sim$1800 cm$^{-1}$ (despite the interference from solvent background) and $\sim$1000 cm$^{-1}$, corresponding to electronic transitions between the first ($S_{11}$) and second ($S_{22}$) van Hove singularity pairs in semiconducting SWNTs, respectively (Fig. 1(a)). The first electronic transition of metallic SWNTs ($M_{11}$) could also be detected at $\sim$700 cm$^{-1}$ (Fig. 1(a)). The observation of these characteristic absorption features is consistent with the expectation that the functionalization of SWNTs targets the defect-derived carboxylic acid moieties on the nanotube surface. This mode of functionalization is known to preserve the electronic absorption properties of SWNTs [21].

It is known that SWNTs without functionalization may be dispersed into polar solvents with the aid of surfactants or polymers such as poly(phenylene vinylene) [22] and poly(vinyl pyrolidone) [8], due presumably to non-covalent interactions. The polyimide CP-2 is somewhat special in this regard [11], such that SWNTs are readily suspended in a DMF solution of CP-2, and the suspension appears homogeneous. The absorption spectrum of the suspended SWNTs is also shown in Fig. 1. However, while the suspension is stable and looks similar to the solution of the functionalized sample PI-$NH_2$–SWNT (similar absorption spectra as well, Fig. 1(a)), the molecular level structures and properties of the suspended and functionalized SWNTs must be different. A clear indication for such difference is in the results of nanotube photoluminescence, which is associated with passivated surface defects in exfoliated carbon nanotubes [6,16,23–25]. As compared in

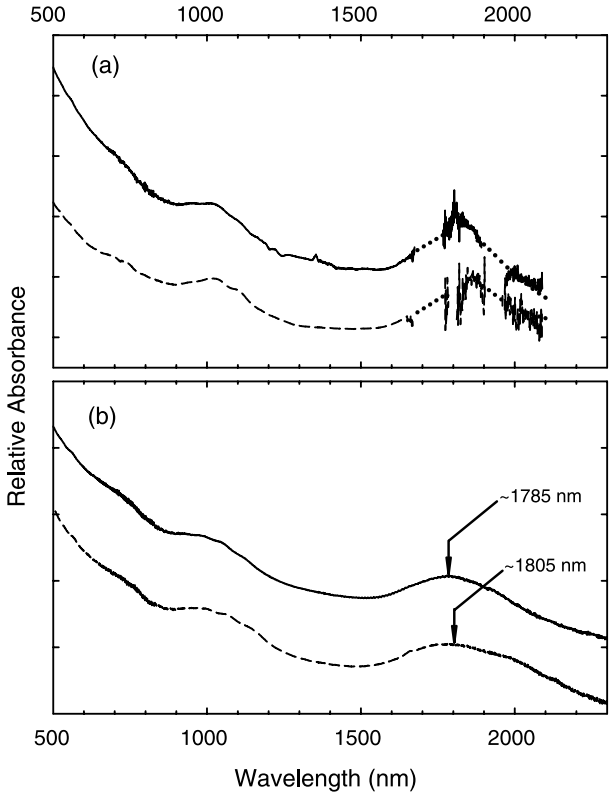


Fig. 1. (a) Optical absorption spectra of PI-$NH_2$–SWNT in DMF solution (—) and polyimide-assisted SWNT suspension in DMF (- - -). (b) Optical absorption spectra of nanocomposite films from the functionalized (—) and suspended (- - -) SWNTs.

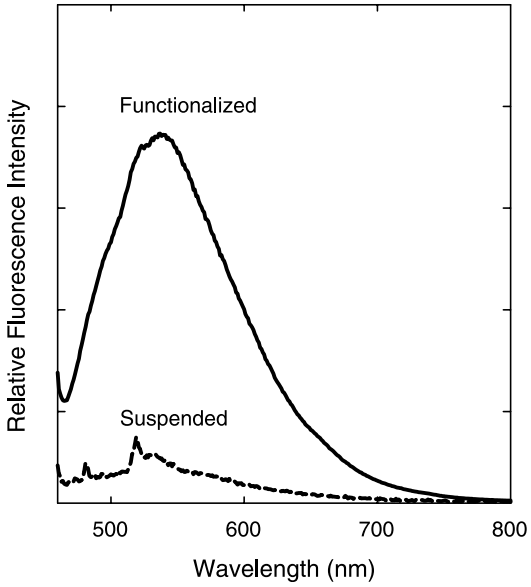


Fig. 2. Luminescence emission spectra (450 nm excitation) of PI-$NH_2$–SWNT in DMF solution (—) and polyimide-assisted SWNT suspension in DMF (- - -).

Fig. 2, the PI-$NH_2$–SWNT solution in DMF is strongly photoluminescent, whereas the apparently stable polyimide-assisted suspension of purified SWNTs in the same solvent with the same optical density at the excitation wavelength is hardly emissive. This is understandable because there is obviously a lack of passivation effect for surface defects in the suspended nanotubes, and the nanotubes in suspension are bundled (thus significant inter-tube quenching of photoexcited states) [16,23,26]. The difference in molecular level structures and properties between the functionalized and suspended SWNTs may represent a primary factor in the dispersion of the nanotubes in polymeric matrix.

### 3.2. Nanocomposite films

The solution of PI-$NH_2$–SWNT and the suspension of purified SWNTs, both in DMF, were used in the fabrication of polyimide (CP-2)–SWNT nanocomposite films via wet-casting. The fabrication procedures were largely similar between the two samples (except for the homogenization and sonication required for the suspended SWNTs), and the resulting films also appeared similar. Since the nanotube contents in the functionalized and suspended samples were known (from quantitative $^1$H NMR signal integration [18] and the amount of added nanotubes, respectively), the nanotube contents in the resulting nanocomposite films were obtained by quantifying the amount of blank CP-2 polymer used in the preparation of the mixtures for wet-casting. The films from both the functionalized and suspended nanotube samples appeared similarly optically transparent when the nanotube loading was low or the films were ultra-thin.

The color of the films was dependent on the nanotube content and also the film thickness. The films with higher nanotube contents appeared black. For a better comparison, the two kinds of films obtained from the functionalized and suspended nanotube samples were controlled to the nanotube loading of 1% by weight and a similar thickness of about 80 μm. As shown in Fig. 1(b), optical absorption spectra of both films exhibit the characteristic $S_{11}$ (around 1800 nm) and $S_{22}$ (around 1000 nm) bands for semiconducting SWNTs and also the $M_{11}$ absorption (around 700 nm) for metallic SWNTs, similar to those of the PI-$NH_2$–SWNT solution and suspended SWNTs in DMF (Fig. 1(a)). These spectral features confirm the expected preservation of electronic structures for the SWNTs embedded in the CP-2 polymer matrix.

In a closer examination of the absorption spectra, the $S_{11}$ and $S_{22}$ bands of the film with functionalized SWNTs are somewhat narrower in bandwidth than those of the film with suspended SWNTs, and the former are also slightly blue-shifted (Fig. 1(b)). These subtle changes in absorption spectral features are consistent with the improved dispersion of the functionalized SWNTs in the polymer matrix. As proposed in the literature [27], van der Waals interactions between nanotubes in a bundle help the overlap between electronic transition states and reduce the band gap of the nanotubes. Therefore, the exfoliation of bundled SWNTs brought about by functionalization gives rise to a better dispersion in the nanocomposite film resulting in narrower and blue-shifted band gap absorption bands.

The improved dispersion of the functionalized SWNTs in the nanocomposite film is reflected by the observation of strong photoluminescence in the visible (Fig. 3), as it is known that the nanotube defect-derived luminescence emission is sensitive to the exfoliation and surface passivation of the nanotubes [16]. Generally speaking, a better functionalization of SWNTs means more effective surface passivation of the defect sites and leads to more homogeneous dispersion (less bundling), which correspond to enhanced luminescence emissions with minimized inter-tube quenching [16]. For the film obtained from the suspended SWNTs, although the macroscopic appearance showed no dramatic difference from that of the film with functionalized SWNTs, the nanoscopic structure of the film must be different. The nanotube bundles in the original

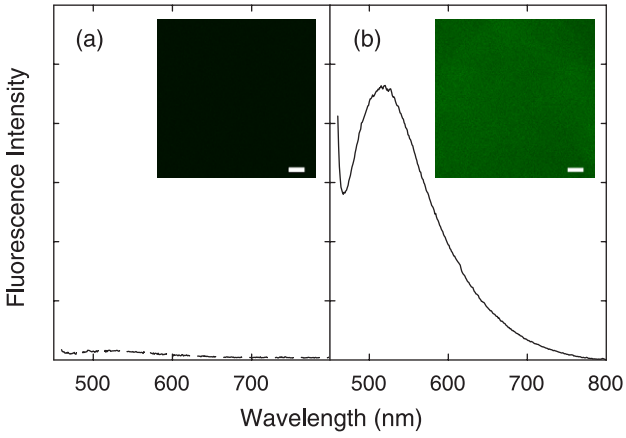


Fig. 3. Luminescence emission spectra (450 nm excitation) of the films from (a) suspended SWNTs and (b) PI-$NH_2$–SWNT. Shown in the insets are corresponding confocal microscopy images of the films (458 nm excitation, >469 nm detection; scale bars = 5 μm).

suspension were likely carried over into the nanocomposite film, and the bundled SWNTs embedded in the CP-2 polymer matrix were essentially non-luminescent (Fig. 3). Therefore, the measurement of defect-derived luminescence emissions serves as a convenient and non-destructive technique in the evaluation and analysis concerning the degree of nanotube dispersion in polymeric nanocomposites qualitatively or even quantitatively (by comparing different films or the use of standards).

The strong photoluminescence in functionalized nanotube samples is known to interfere with Raman analyses of these samples in an overwhelming fashion [6]. In fact, the better the nanotube functionalization and dispersion, the stronger the interference becomes. The Raman results on the two kinds of polyimide (CP-2)–SWNT nanocomposite films were as expected. For the film with functionalized SWNTs, the nanotube Raman signals could be detected only with the use of lower laser power at the expense of sensitivity, making the characteristic features of SWNTs poorly defined on top of a huge luminescence background in the observed Raman spectrum (Fig. 4). This is consistent with the film being strongly photoluminescent, as discussed above (Fig. 3). The film with suspended SWNTs, on the other hand, was non-luminescent, so that characteristic Raman features of the embedded SWNTs were clearly observed. With a subtraction of the luminescence background, the G-band and D*-band features for functionalized SWNTs in the film can be identified at 1593 and 2642 $cm^{-1}$, respectively, which are at slightly higher frequencies than those for the suspended SWNTs in film (1587 and 2631 $cm^{-1}$, respectively). Therefore, it might be argued that there is the commonly acknowledged enhancement in polymer–nanotube interactions [13–15] in the film with functionalized SWNTs. With probably similar effect, the radial breathing mode (RBM) feature at 179 $cm^{-1}$ for the film with functionalized nanotubes is also at a slightly higher frequency than that of the film with suspended nanotubes (170 $cm^{-1}$).

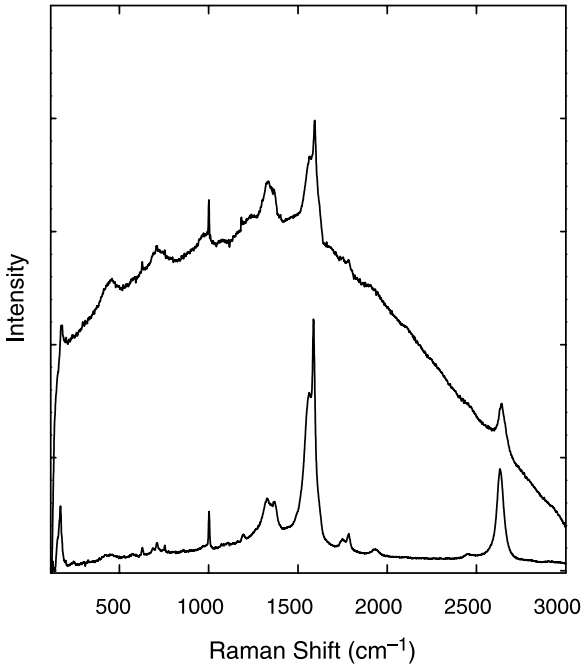


Fig. 4. Raman spectra (633 nm excitation) of the films with PI-$NH_2$–SWNT (top) and suspended SWNTs (bottom). Some small peaks in the spectra are due to imperfect correction for the polyimide signals.

In order to allow a more direct evaluation on the nanotube dispersion in the films, microtome technique was employed to obtain ultra-thin (about 100 nm) slices. An SEM image for a slice from the film with functionalized SWNTs is shown in Fig. 5, which seems consistent with a well-dispersion of the nanotubes in the film. The slice was also evaluated by using high-resolution TEM. The specimen was highly sensitive to the electron beam, which instantly created nanoscopic gaps in the film slice. There were mostly individual SWNTs bridging the gaps, as shown in Fig. 5. However, for the film with suspended SWNTs, the slices from microtome were of poor quality, inadequate for any conclusive SEM and TEM analyses.

Alternatively, the polyimide nanocomposite films with the functionalized and suspended SWNTs were both stretched to failure, and the fracture edges were examined by using SEM for the morphological characteristics (generally reflecting the

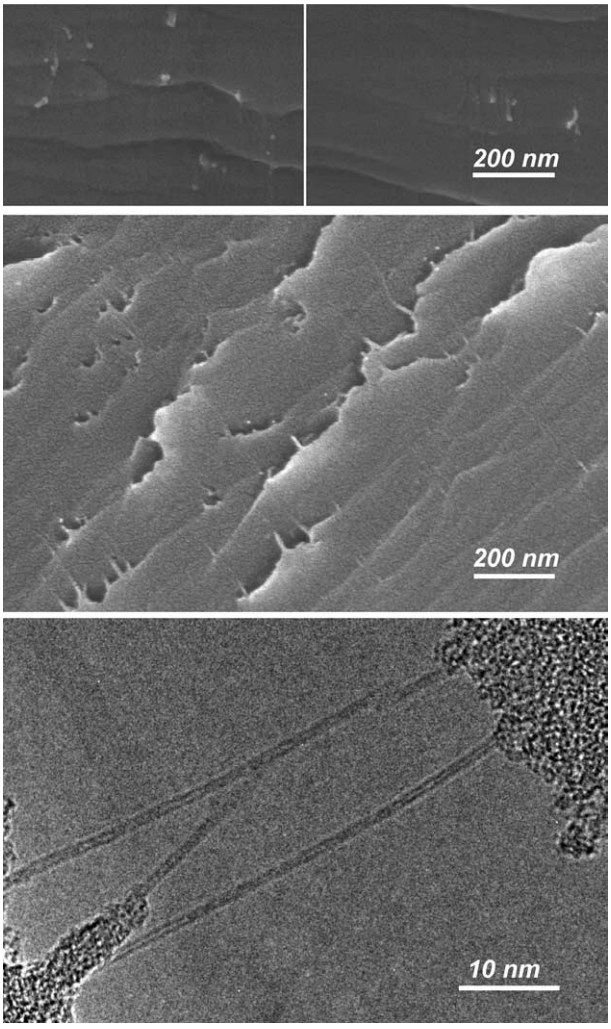


Fig. 5. Results from electron microscopy analyses of the films with suspended SWNTs (top: SEM images of a slice from microtome) and with PI-$NH_2$–SWNT (middle: SEM image of a slice from microtome; and bottom: TEM image of the specimen with a gap generated by the electron beam).

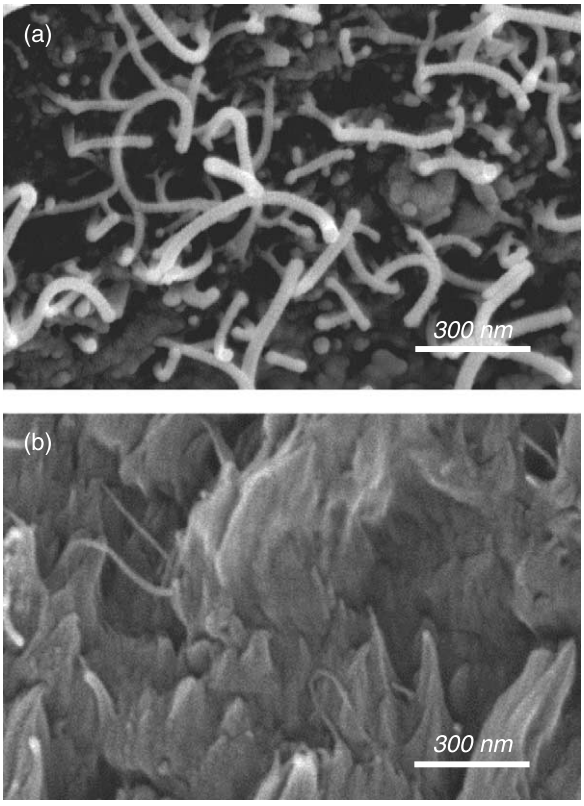


Fig. 6. SEM images on fracture edges of the films (stretched to failure) with (a) suspended SWNTs and (b) PI-$NH_2$–SWNT.

nanotube dispersion and load transfer efficiency in the films) [28,29]. As shown in Fig. 6, the fracture surface morphology is different between the two films. For the film from suspended SWNTs, there are plenty of exposed nanotube thick bundles on the fracture surface (the appearance of more nanotubes than what might be expected from the film composition probably due primarily to the nanotube bundles being pulled out of the polymer matrix in the stretching and also to inhomogeneous distributions of nanotubes in the film). This is obviously not the case at the fracture edge of the film from functionalized SWNTs. Despite the same overall nanotube loading, the homogeneous dispersion and better polymer wetting of functionalized SWNTs in the film are likely responsible for the apparently different fracture surface morphology (Fig. 6).

In summary, the polyimide–SWNT nanocomposite thin film prepared from polyimide-functionalized SWNTs was compared to that from purified SWNTs in polyimide-assisted suspension. At the same nanotube contents and film thicknesses, the visual appearance was hardly different between the two kinds of films. However, the nanotube dispersion must be significantly better in the film with functionalized SWNTs, as reflected by the strong photoluminescence in the luminescence emission spectroscopy and confocal microscopy results of the film. The results from other characterization techniques including optical absorption, Raman, and electron microscopy are consistent with the conclusion on the better dispersion of functionalized SWNTs in the film for improved compatibility with the matrix polymer and more efficient load transfer. Further studies to compare the two kinds of films for more specific material properties (such as mechanical [28], thermal, and electrical) and performance should be interesting.

## Acknowledgements

We thank Dr Yang Liu, Dr. Haifang Wang, and Jennifer Roberts for experimental assistance. Financial support from NASA (through a cross-enterprise NRA), NSF, Center for Advanced Engineering Fibers and Films (NSF-ERC at Clemson University), and Office of Naval Research is gratefully acknowledged. D.E.H. was an awardee of the NASA Graduate Student Researcher Program (GSRP). J.D. was a participant of the Research Experience for Undergraduates (REU) program sponsored jointly by NSF and Clemson University. Research at Oak Ridge National Laboratory was sponsored by the Assistant Secretary for Energy Efficiency and Renewable Energy, Office of FreedomCAR and Vehicle Technologies, as part of the HTML User Program, managed by UT-Battelle LLC for DOE.

## References

[1] Ajayan PM. Chem Rev 1999;99(7):1787–99.
[2] Baughman RH, Zakhidov AA, de Heer WA. Science 2002;297(5582):787–92.
[3] Tasis D, Tagmatarchis N, Bianco A, Prato M. Chem Rev 2006;106(3):1105–36.
[4] Mitchell CA, Bahr JL, Arepalli S, Tour JM, Krishnamoorti R. Macromolecules 2002;35(23):8825–30.
[5] Hill DE, Lin Y, Rao AM, Allard LF, Sun YP. Macromolecules 2002;35(25):9466–71.
[6] Sun YP, Fu K, Lin Y, Huang W. Acc Chem Res 2002;35(12):1096–104.
[7] Lin Y, Zhou B, Fernando KAS, Liu P, Allard LF, Sun YP. Macromolecules 2003;36(19):7199–204.
[8] O'Connell MJ, Boul P, Ericson LM, Huffman C, Wang YH, Haroz E, et al. Chem Phys Lett 2001;342(3-4):265–71.
[9] Moore VC, Strano MS, Haroz EH, Hauge RH, Smalley RE. Nano Lett 2003;3(10):1379–82.
[10] Lin Y, Taylor S, Li H, Fernando KAS, Qu L, Wang W, et al. J Mater Chem 2004;14(4):527–41.
[11] Delozier DM, Watson KA, Smith JG, Clancy TC, Connell JW. Macromolecules 2006;39(5):1731–9.
[12] Ajayan PM, Stephan O, Colliex C, Trauth D. Science 1994;265(5176):1212–4.
[13] Lourie O, Wagner HD. J Mater Res 1998;13(9):2418–22.
[14] Hadjiev VG, Iliev MN, Arepalli S, Nikolaev P, Files BS. Appl Phys Lett 2001;78(21):3193–5.
[15] Liu J, Liu T, Kumar S. Polymer 2005;46(10):3419–24.
[16] Lin Y, Zhou B, Martin RB, Henbest KB, Harruff BA, Riggs JE, et al. J Phys Chem B 2005;109(31):14779–82.
[17] Hill DE, Lin Y, Qu L, Kitaygorodskiy A, Connell JW, Allard LF, et al. Macromolecules 2005;38(18):7670–5.
[18] Qu L, Lin Y, Hill DE, Zhou B, Wang W, Sun X, et al. Macromolecules 2004;37(16):6055–60.
[19] Sen R, Rickard SM, Itkis ME, Haddon RC. Chem Mater 2003;15(22):4273–9.
[20] Haddon RC, Sippel J, Rinzler AG, Papadimitrakopoulos F. MRS Bull 2004;29(4):252–9.
[21] Niyogi S, Hamon MA, Hu H, Zhao B, Bhowmik P, Sen R, et al. Acc Chem Res 2002;35(12):1105–13.
[22] (a) Curran SA, Ajayan PM, Blau WJ, Carroll DL, Coleman JN, Dalton AB, et al. Adv Mater 1998;10(14):1091–3.

(b) Star A, Stoddart JF, Steuerman D, Diehl M, Boukai A, Wong EW, et al. Angew Chem Int Ed 2001;40(9):1721–5.
[23] Riggs JE, Guo Z, Caroll DL, Sun YP. J Am Chem Soc 2000;122(24): 5879–80.
[24] Sun YP, Zhou B, Henbest K, Fu K, Huang W, Lin Y, et al. Chem Phys Lett 2002;351(5-6):349–53.
[25] Zhou B, Lin Y, Veca LM, Ferando KAS, Harruff BA, Sun YP. J Phys Chem B 2006;110(7):2001–6.
[26] O'Connell MJ, Bachilo SM, Huffman CB, Moore VC, Strano MS, Haroz EH, et al. Science 2002;297(5581):593–6.
[27] Graff RA, Swanson JP, Barone PW, Baik S, Heller DA, Strano MS. Adv Mater 2005;17(8):980–4.
[28] Ajayan PM, Schadler LS, Giannaris C, Rubio A. Adv Mater 2000;12(10): 750–3.
[29] Paiva MC, Zhou B, Fernando KAS, Lin Y, Kennedy JM, Sun YP. Carbon 2004;42(14):2849–54.